Replication Report: Discovering governing equations from data: Sparse identification of nonlinear dynamical systems (SINDy)

An Applied Intelligence replication run, Claude Code driving the released harness

2026-07-03

1 Overview

This report documents a replication of the core low-dimensional computational claims of Brunton, Proctor & Kutz, "Discovering governing equations from data: Sparse identification of nonlinear dynamical systems" (arXiv:1509.03580), executed through the paper-replication harness of Hans & Bilionis (arXiv:2607.02134). Eleven targets were planned covering Examples 1, 2, and 4 of the paper (simple illustrative systems, the Lorenz system, and bifurcations/normal forms). Example 3 (cylinder wake) was deliberately excluded from the target plan: it requires DNS-derived data unavailable in this replication environment. All method components (polynomial candidate library, sequentially thresholded least squares, derivative-noise model, total-variation-regularized derivative, discrete-time formulation, bifurcation-parameter suspension) were reconstructed from the paper text alone; no author code was used. Random seeds necessarily differ from the original study; all numeric tolerances were pre-registered in target configs before the first run.

2 Targets

2.1 Example 1: simple illustrative systems

term	$\dot{x}$ (ours)	$\dot{x}$ (paper)	$\dot{y}$ (ours)	$\dot{y}$ (paper)
x	-0.1002	-0.1015	-2.0005	-1.9990
y	1.9994	2.0027	-0.0988	-0.0994

Table 1: Damped harmonic oscillator with linear terms: identified nonzero coefficients vs. the paper's Tab:Ex1_2dLin values.

term	$\dot{x}$ (ours)	$\dot{x}$ (paper)	$\dot{y}$ (ours)	$\dot{y}$ (paper)
xxx	-0.0979	-0.0996	-2.0003	-1.9994
yyy	2.0017	1.9970	-0.1004	-0.0979

Table 2: Damped harmonic oscillator with cubic nonlinearity vs. Tab:Ex1_2dCub.

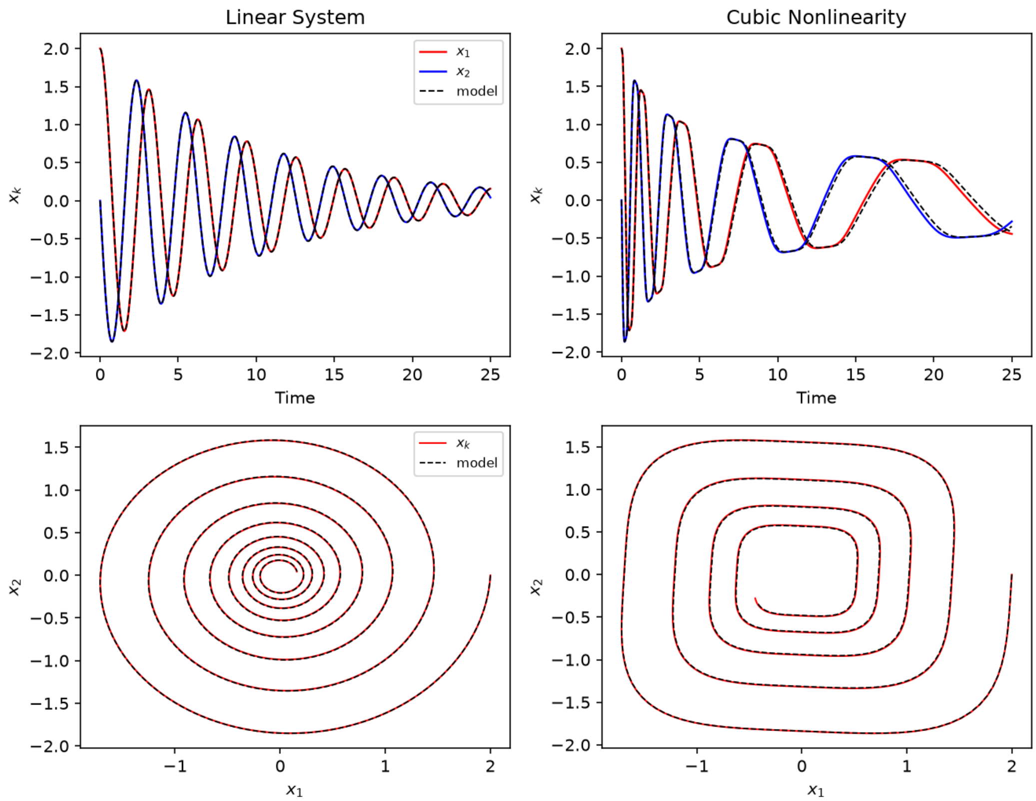

Figure 1: Reproduction of Fig:Ex1: trajectories and phase portraits of the linear (left) and cubic (right) 2D damped oscillators; identified models dashed black.

term	$\dot{x}$ (ours)	$\dot{x}$ (paper)	$\dot{y}$ (ours)	$\dot{y}$ (paper)	$\dot{z}$ (ours)	$\dot{z}$ (paper)
x	-0.1006	-0.0996	-1.9985	-1.9997	0	0
y	2.0011	2.0005	-0.1005	-0.0994	0	0
z	0	0	0	0	-0.3026	-0.3003

Table 3: Three-dimensional linear system vs. Tab:Ex1_3d.

2.2 Example 2: Lorenz system

term	$\dot{x}$ (ours)	$\dot{x}$ (paper)	$\dot{y}$ (ours)	$\dot{y}$ (paper)	$\dot{z}$ (ours)	$\dot{z}$ (paper)
x	-10.0005	-9.9996	27.9999	27.9980	0	0
y	10.0002	9.9998	-1.0002	-0.9997	0	0
z	0	0	0	0	-2.6669	-2.6665
xy	0	0	0	0	1.0000	1.0000
xz	0	0	-1.0000	-0.9999	0	0

Table 4: Lorenz system identified at derivative-noise level $\eta = 1.0$ vs. the paper's appendix table ($\sigma = 10$, $\rho = 28$, $\beta = 8/3$).

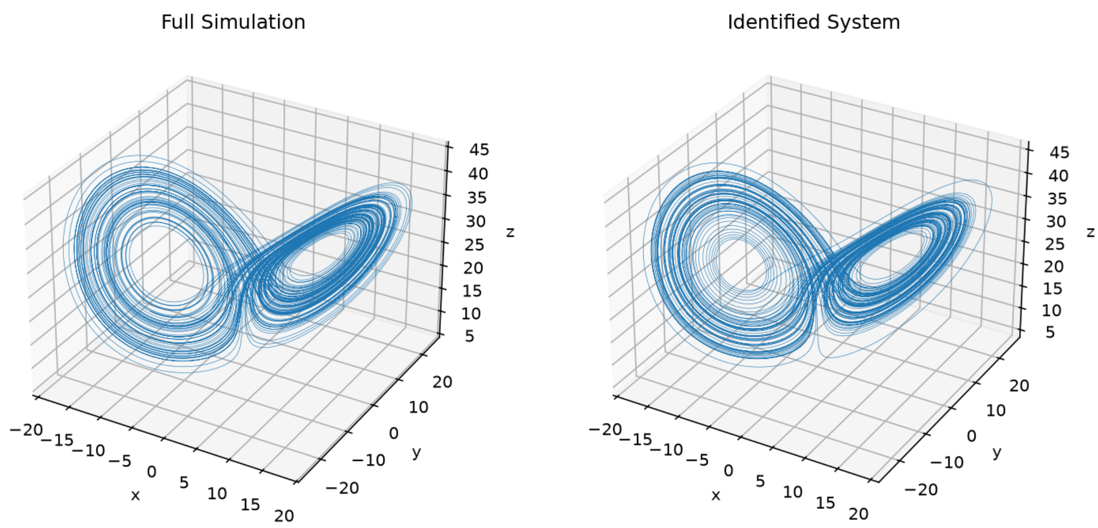

Figure 2: Lorenz attractor: full simulation vs. identified system (both from $x_0 = (-8, 7, 27)$). The identified model preserves the two-lobed attractor geometry.

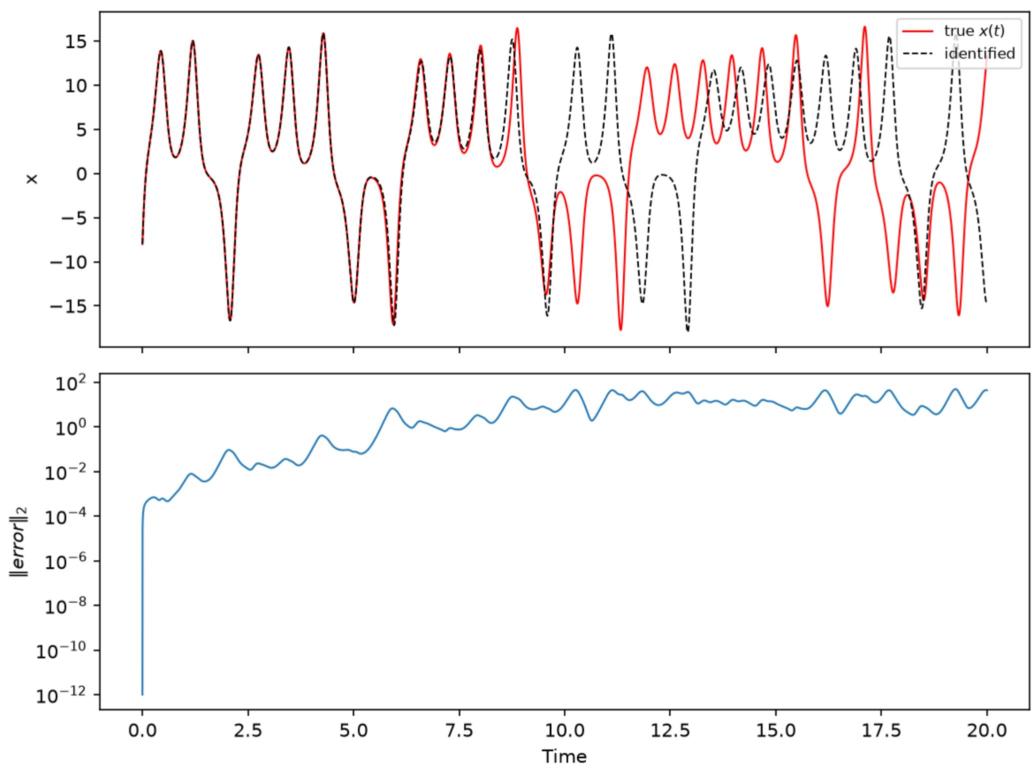

Figure 3: Short-term tracking and long-term divergence of the identified Lorenz model: accurate prediction over short horizons, exponential separation thereafter (chaos), with the trajectory remaining on the attractor.

2.3 Example 4: bifurcations and normal forms

term	x_{k+1} (ours)	x_{k+1} (paper)	r_{k+1} (ours)	r_{k+1} (paper)
r	0	0	1.0000	1.0000
xr	0.9996	0.9993	0	0
xxr	-0.9995	-0.9989	0	0

Table 5: Logistic map identified with discrete-time SINDy vs. Tab:Logistic.

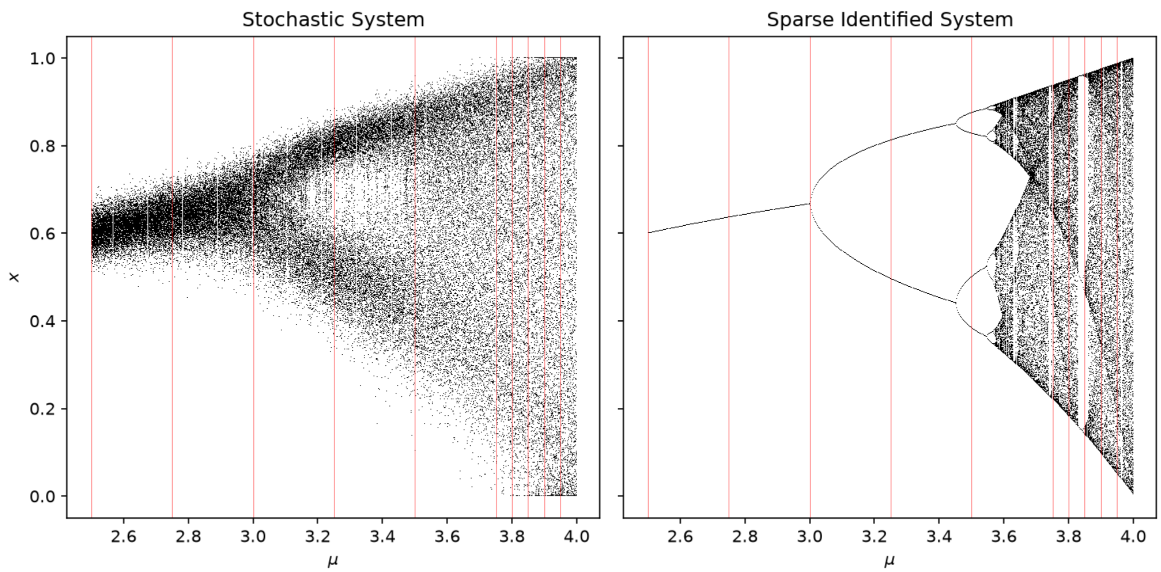

Figure 4: Reproduction of Fig:Logistic: attracting sets of the stochastically forced logistic map (left) and of the sparse identified map (right); sampled μ rows in red.

term	$\dot{x}$ (ours)	$\dot{x}$ (paper)	$\dot{y}$ (ours)	$\dot{y}$ (paper)	$\dot{u}$ (ours)	$\dot{u}$ (paper)
x	0	0	0.9998	0.9914	0	0
y	-0.9997	-0.9920	0	0	0	0
xu	0.9918	0.9269	0	0	0	0
yu	0	0	0.9965	0.9294	0	0
xxx	-0.9916	-0.9208	0	0	0	0
xxy	0	0	-0.9958	-0.9244	0	0
xyy	-0.9919	-0.9211	0	0	0	0
yyy	0	0	-0.9965	-0.9252	0	0

Table 6: Hopf normal form identified from sensor-noise data with TV-regularized derivatives vs. Tab:Hopf. The paper's own cubic coefficients deviate ∼8% from truth; acceptance is anchored to truth with tolerance 0.12.

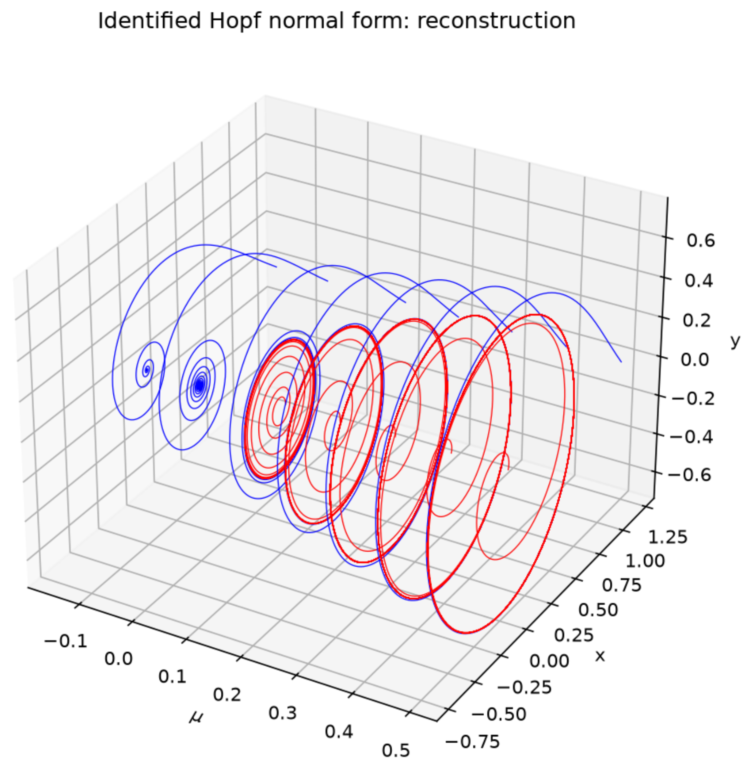

Figure 5: Reproduction of Fig:HopfReconstruct: the identified model produces a stable fixed point for $\mu < 0$ and a limit cycle of radius $\approx \sqrt{\mu}$ for $\mu > 0$.

3 Notes

Deviations and residual gaps: Example 3 (cylinder wake) not planned (no DNS data in this environment); setup values not stated in the paper (integration spans, noise magnitudes for Example 1, thresholds λ, Hopf training grid, TV parameters) are recorded as explicit hypotheses in `spec/assumptions_and_unknowns.md` and in each target config. The Hopf rotation sense follows the signs of Tab:Hopf ($\omega = -1$ convention). Hardware: Apple M-series laptop, single process; per-target runtimes range from seconds (Example 1) to a few minutes (Lorenz at $dt = 10^{-3}$ over $T = 100$, Hopf TV differentiation). Full per-target numeric evidence lives in `artifacts/*/*.metrics.json`; provenance and run ledger under `artifacts/provenance/` and `artifacts/runs/`.